

Magneto-Optical Kerr Spectroscopy of a New Chemically Ordered Alloy: Co_3Pt

G. R. Harp, D. Weller, T. A. Rabedeau, R. F. C. Farrow, and M. F. Toney
IBM Almaden Research Center, 650 Harry Road, San Jose, California 95120-6099

(Received 14 June 1993)

The sensitivity of magneto-optical spectra to alloy chemical ordering is established. This is demonstrated for a new ordered Co_3Pt phase, which was synthesized in thin film form using molecular beam epitaxial growth. This compound consists of alternating planes of Co and CoPt atoms with a hexagonal $ABAB\dots$ layer sequence. The chemical ordering is accompanied by a substantial electronic structure change as reflected in a new peak in magneto-optical spectra at ~ 3.2 eV photon energy.

PACS numbers: 78.20.Ls, 61.66.Dk, 81.30.Bx

Magneto-optical effects have attracted a lot of attention recently in research of magnetic thin films and multilayers. Strong resonance effects due to reduced optical constants [1,2], quantum confinement effects in ultrathin Fe layers [3], oscillations of the Kerr rotation with magnetic layer thickness due to quantum well states [4,5] and strong correlations between the magneto-optical Kerr effect (MOKE), and magnetic anisotropies [6] are among the most exciting recent discoveries in this field. While magnetostructural correlations have been known for a long time [7], the possibility of chemical ordering-related effects in the magneto-optical spectra has been suggested only recently [8,9]. With the advent of improved band-structure-based magneto-optical calculations [10], it is possible to understand magneto-optical transitions from first principles and predict the effects of material structure upon Kerr rotation. In particular, the effect of chemical ordering on magneto-optical properties provides an important test of current theory. Co-Pt alloys provide an attractive candidate material for such studies since the Co-Pt bulk phase diagram reveals a continuous series of solid solutions with ferromagnetic order up to 90 at. % Pt at room temperature and the existence of chemically ordered CoPt and CoPt_3 phases [11]. No chemically ordered compound is known for the composition Co_3Pt [11], although an $L1_2$ cubic phase has been predicted in a recent calculation by Sanchez *et al.* [12]. In this Letter we report the observation of a chemically ordered Co_3Pt structure in films grown by molecular beam epitaxy (MBE). More importantly, we report the first unambiguous correlation between chemical ordering and magneto-optical Kerr rotation.

1000 Å thick $\text{Co}_{77}\text{Pt}_{23}$ alloy films were deposited by MBE at various temperatures onto 10 Å Pt buffer layers which were grown at 875 K on sapphire (0001) substrates. This results in high quality (111) [or (0001)] oriented alloy films [13]. The deposition chamber was maintained at a pressure $< 4 \times 10^{-10}$ mbar throughout growth. Electron gun sources were used for both Co and Pt, with deposition rates in the range 0.05–0.2 Å/s. All compositions were checked with x-ray fluorescence. The spectral dependences of the polar Kerr effect were measured in saturating fields of ± 20 kOe in the photon energy

range 0.8–5.3 eV [14]. The saturation magnetization was determined using vibrating sample magnetometry. All magnetic and magneto-optic measurements were made at room temperature.

A series of MOKE spectra of Co_3Pt films, grown at various temperatures, are displayed in Fig. 1. All films had the same room temperature magnetization of 970 emu/cc within experimental error ($\pm 5\%$). The curve at 950 K and another measurement at 750 K (not shown) are similar to previous measurements [8] of chemically disordered fcc Co_3Pt alloys. Below 700 K the spectra undergo a drastic change and a new peak near 3.2 eV emerges. No indications of optical constant modifications were evident from reflectivity measurements with 0.8–5.3 eV photons. Rather, this new feature in the Kerr spectra is associated with a change in the spin-polarized electronic structure of these alloys. Taking the area be-

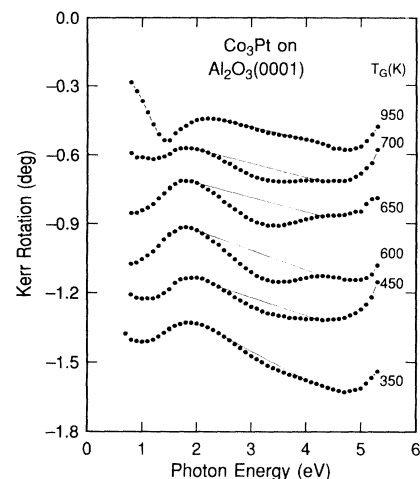


FIG. 1. Energy dependent polar magneto-optical Kerr spectra from $\text{Co}_{77}\text{Pt}_{23}$ (Co_3Pt) films deposited at various temperatures. Above 750 K, the spectra are temperature independent, and represent a chemically disordered fcc Co_3Pt phase. Below 750 K, the MOKE spectra change radically, indicating gross changes in the spin-polarized band structure. The 950 K spectrum is to scale; all other spectra are shifted by a constant offset of 0.2° towards each other.

tween the straight line in Fig. 1 and the measured spectra as representative of the strength of the 3.2 eV feature, we find that it is maximal for films grown at 600–650 K. It decays rapidly for films deposited at temperatures outside this optimal range. This, together with structural data discussed below, is summarized in Fig. 4, where the integrated peak area is plotted as a function of the deposition temperature. Besides the development of the new, striking 3.2 eV feature, there are other changes to the MOKE spectra. For example, the 1.5 eV peak of the 950 K film completely vanishes or shifts to lower photon energy out of the measurement range as the growth temperature is lowered to 600–650 K. Also the strength of the ultraviolet peak at 4.8 eV is strongly affected. All these changes in the Kerr spectra suggest accompanying changes in the film structure, the subject to which we now turn.

The structure of a number of films with growth temperatures bracketing those yielding the maximal MOKE 3.2 eV peak area was characterized by x-ray scattering measurements, primarily using a rotating anode source. The scattering data confirm the films to be epitaxial with the growth axis corresponding to fcc (111) or hcp (0001) depending on the deposition temperature. Figure 2 depicts scattering data collected as a function of surface normal momentum transfer (q_z) with the in-plane momentum transfer ($q_{||}$) fixed at $4\pi/a\sqrt{3} \text{ \AA}^{-1}$ where a is the in-plane nearest neighbor separation 2.6 Å (see in-

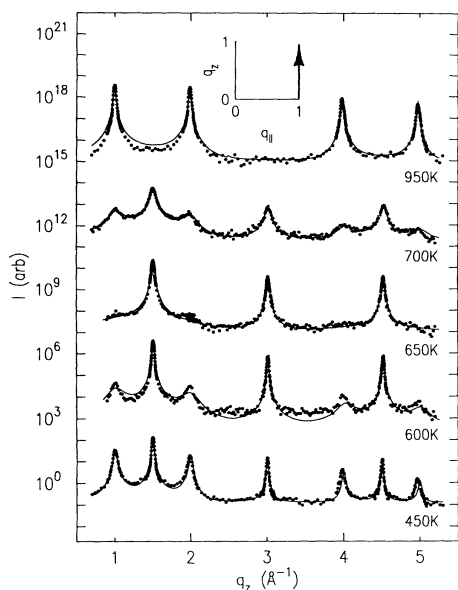


FIG. 2. Scattering along a ($10q_z$) trajectory through reciprocal space for five samples. The in-plane momentum transfer is fixed at 1.0 reciprocal lattice unit ($4\pi/a\sqrt{3} \text{ \AA}^{-1}$) while the surface-normal momentum transfer q_z is varied (see inset). Peaks at $q_z = 1, 2, 4, 5 \text{ \AA}^{-1}$ result from fcc stacking while those at $q_z = 1.5n \text{ \AA}^{-1}$ stem from hcp stacking. The lines represent the results of fits to the layer stacking model of Ref. [15].

set). These scans permit differentiation of an fcc stacking sequence ($ABCABC\dots$) from an hcp layer sequence ($ABAB\dots$) as hcp stacking yields peaks at $q_z = 1.5n \text{ \AA}^{-1}$ (n an integer) while twinned fcc stacking results in peaks at $q_z = 1, 2, 4, 5, \dots \text{ \AA}^{-1}$. The fraction of the film with fcc stacking was extracted by fitting the scattering data to the calculated scattering of a model structure incorporating hcp stacking with correlated stacking faults resulting in fcc inclusions [15]. The results of these fits are depicted as the solid lines in Fig. 2 and the fcc fractions are listed in Table I. At the lowest temperatures the stacking is largely hcp with a high concentration of clustered stacking faults resulting in $\sim 35\%$ local fcc stacking. As the deposition temperature increases the density of stacking faults is reduced resulting in excellent hcp stacking for the samples grown at 600 and 650 K. Further increases in deposition temperature result in a transition from hcp to fcc stacking. A similar hcp to fcc transition near 700 K is well known in bulk Co-Pt alloys for Pt concentrations up to 20 at.% [11,16].

Specular data are presented in Fig. 3. In addition to the expected peaks at $3.0n \text{ \AA}^{-1}$, which are present in both fcc and hcp structures, specular data of the lower temperature (hcp) films manifest additional peaks at $1.5n \text{ \AA}^{-1}$. These peaks (forbidden in a disordered hcp alloy) indicate the Co_3Pt alloy is chemically ordered along the normal with A and B layers possessing *differing stoichiometry*. Using the integrated area of the specular peaks in a structure factor calculation (assuming hcp structure) yields the A and B layer Pt fractions listed in Table I. Examination of this table reveals that the greatest Pt segregation to layer B is obtained for the films with the fewest fcc inclusions. For these films the surface-normal chemical correlation length is only slightly less than the structural correlation length (see Table I). We

TABLE I. Structural characteristics extracted from x-ray scattering data. Pt A and B are the Pt fractional occupancies ($\pm 1\%$) of layers A and B based on structure factor calculations. (Overall film stoichiometry was determined to be slightly Co rich by fluorescence analysis.) S is the alloy one-dimensional chemical order parameter. $(c/a)^*$ denotes the deviation of the actual c/a ratio from the ideal hcp value of $\sqrt{8/3}$ or fcc ratio (950 K film) of $\sqrt{6}$. $\xi_{s\perp}$ is the structural coherence length along the surface normal (1/HWHM of specular peak at 3.0 \AA^{-1}) while $\xi_{c\perp}$ is the alloy chemical coherence length along the normal (1/HWHM of the specular peak at 1.5 \AA^{-1}). Note that $\xi_{c\perp}$ is independent of the alloy in-plane order. Typical surface normal and in-plane mosaics are 0.5° and 1.0° , respectively.

Growth Temp. (K)	Pt A (%)	Pt B (%)	S	$(c/a)^*$	fcc portion (%)	$\xi_{s\perp}$ (Å)	$\xi_{c\perp}$ (Å)
450	19.2	26.4	0.14	0.987	35.6	200	130
600	7.1	38.5	0.63	0.982	8.34	180	170
650	8.0	38.4	0.61	0.980	<5.0	190	110
700	16.2	31.0	0.30	0.981	27.5	200	30
950	0.992	>99.0	150	...

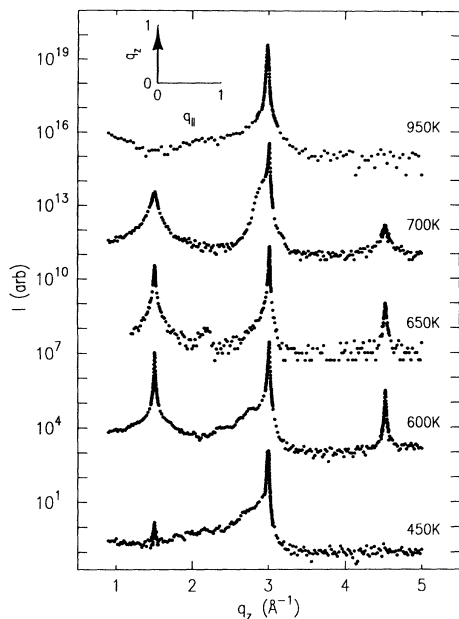


FIG. 3. Specular data collected for the five samples depicted in Fig. 2. The peaks at 3.0 \AA^{-1} are observed for either fcc or hcp stacking. The peaks at 1.5 and 4.5 \AA^{-1} result from alloy ordering such that A and B layers have differing stoichiometries. The asymmetry of the peaks at 3.0 \AA^{-1} results from sapphire and Pt buffer layer scattering. The inset depicts the trajectory through reciprocal space.

assume that the reduced Pt segregation and increase in fcc stacking in the lower temperature films stem from kinetic limitations on ordering during growth rather than reentrant fcc phase stability.

The existence of chemical ordering along the film normal suggests the possibility of in-plane chemical ordering. A synchrotron study of the sample deposited at 650 K reveals a series of peaks consistent with in-plane doubling of the unit cell [17]. These peaks are broad, however, indicating short chemical correlation lengths. Explicitly, the in-plane chemical correlation length (peak inverse half width at half maximum, $1/\text{HWHM}$) is only $\sim 8 \text{ \AA}$. Thus we cannot definitively identify the ideal three-dimensional ordered alloy structure, but it is clear that along the (0001) direction the ordered alloy may be regarded as a natural superlattice consisting of alternating Co and CoPt layers.

The hcp \leftrightarrow fcc phase transition in bulk Co-Pt is martensitic (i.e., occurs by collective motions of large groups of atoms), and as a result the phase transition from hcp \rightarrow fcc (increasing temperature) occurs at a higher temperature than the inverse transition from fcc \rightarrow hcp (decreasing temperature) [18]. Beyond 13–20 at. % Pt bulk hcp Co-Pt alloys have not been previously observed [11,16]. One anticipates that in the absence of bulk kinetic limitations one might observe an “equilibrium” transformation temperature (T_{eq}) intermediate between the fcc \rightarrow hcp and hcp \rightarrow fcc transition temperatures. It is

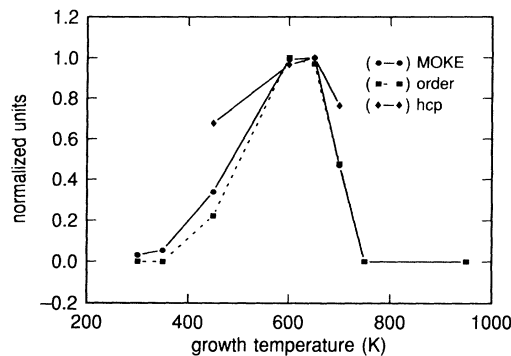


FIG. 4. Normalized MOKE peak area as defined in Fig. 1, hcp fraction, and chemical order parameter as a function of the deposition temperature for MBE deposited $\text{Co}_{77}\text{Pt}_{23}$ (Co_3Pt) alloy films.

this equilibrium temperature which is relevant to MBE deposition since films are constructed atom by atom *directly* into their most stable crystal phase [19]. Hence, we discover that hcp Co_3Pt is the preferred state for low-temperature deposition, even though quenched high-temperature deposited fcc films remain fully fcc at room temperature. We find T_{eq} to be $\approx 650 \text{ K}$ in Co_3Pt , as seen in Fig. 2. This temperature lies in between the extrapolated fcc \rightarrow hcp and hcp \rightarrow fcc transition temperatures in the bulk alloy [11]. Thus, MBE promotes chemical ordering in these alloys relative to conventional ordered alloy production techniques. Bulk ordered alloys are typically prepared at high temperature (disordered state) and then slowly cooled below the order-disorder transition temperature to induce chemical ordering. In contrast, with MBE it is not necessary to depend upon a kinetically limited phase transition to occur. In this way, we find that MBE opens an avenue to the exploration of a new class of lower temperature chemically ordered alloys.

Returning to the issue of correlations between Kerr features and structural characteristics of the film, we note that there are three film structural characteristics that might correlate with the 3.2 eV MOKE peak area: hcp vs fcc stacking (structure), chemical order along the film normal, and uniaxial strain in the film. We plot in Fig. 4 the MOKE peak area as defined above and the hcp fraction of the film (normalized units). While the hcp fraction roughly follows the MOKE peak, the correlation is sufficiently poor to suggest that the peak in the MOKE spectrum is not the result of improved hcp structural perfection. Furthermore, published MOKE spectra of neither hcp Co nor chemically disordered low Pt content hcp Co-Pt alloys (e.g., $\text{Co}_{88}\text{Pt}_{12}$ [20]) show any evidence of the 3.2 eV feature observed for our films. Similarly, the uniaxial strain represented by the c/a values listed in Table I does not correlate well with the MOKE peak area dependence on growth temperature. In contrast, the alloy chemical ordering along the sample normal and the MOKE peak temperature dependence are well correlated. To explore this correlation, we define the one-dimensional

chemical order parameter S [21] presented in Table I. After normalization, these data are also plotted with the MOKE peak area in Fig. 4. The correlation between the MOKE peak area and the alloy chemical order parameter is compelling. Thus we attribute the strong MOKE feature at 3.2 eV to the existence of one-dimensional chemical order. Finally, we note that although this new MOKE feature is present only in the ordered alloy films, there remain other significant differences between the MOKE spectra of the chemically disordered fcc and the chemically disordered predominately hcp films. This is not unexpected, since if the subtle structural changes accompanying chemical ordering can modify MOKE spectra, then clearly the fcc→hcp phase transition should also introduce significant spectral changes.

Considering magneto-optical effects in the framework of a total weight of electronic transitions between initial and final states in the band structure, as introduced by Erskine and Stern [7], we tentatively attribute the new spectral feature to the formation of "localized" electronic states of about 2 eV width, which corresponds to the width of the observed new peak. Independent verification of these states could be made either experimentally, e.g., with spin-polarized electron spectroscopies or theoretically, e.g., with *ab initio* MOKE calculations, based on the structural information that we present in Table I. We expect that similar correlations between MOKE and chemical ordering will be observable in other materials as well.

In summary, we have observed a new Co_3Pt ordered compound. The chemical and structural ordering is accompanied by substantial electronic structure changes as detected with magneto-optical spectroscopy. This new phase is fundamentally different from the as yet unobserved $L1_2$ phase (Au_3Cu analog) predicted by Sanchez *et al.* [12].

We acknowledge stimulating discussions with J. Sticht and H. Brändle. We have benefited from technical support by R.F. Marks, G. Gorman, and R. Savoy. This work was partly funded by the Office of Naval Research (Contract No. N00014-92-C-0084).

-
- [1] T. Katayama, Y. Suzuki, H. Awano, Y. Nishihara, and K. Koshizuka, *Phys. Rev. Lett.* **60**, 1426 (1988); H. Feil and C. Haas, *Phys. Rev. Lett.* **58**, 65 (1987).
 - [2] W. Reim and D. Weller, *Appl. Phys. Lett.* **53**, 2453 (1988).
 - [3] Y. Suzuki, T. Katayama, S. Yoshida, T. Tanaka, and K. Sato, *Phys. Rev. Lett.* **68**, 3355 (1992); Y. Suzuki, T. Katayama, A. Thiaville, K. Sato, M. Taninaka, and S. Yoshida, *J. Magn. Magn. Mater.* **121**, 539 (1993).
 - [4] Y. Suzuki and T. Katayama, *Mater. Res. Soc. Symp. Proc.* **313**, 153–164 (1993).
 - [5] W.R. Bennet, W. Schwarzacher, and W.F. Egelhoff,

- Phys. Rev. Lett.* **65**, 3169 (1990).
- [6] D. Weller, H. Brändle, and C. Chappert, *J. Magn. Magn. Mater.* **121**, 461 (1993).
- [7] J.L. Erskine and E.A. Stern, *Phys. Rev. B* **8**, 1239 (1973).
- [8] D. Weller, H. Brändle, R.F.C. Farrow, R.F. Marks, and G.R. Harp, in *NATO Advanced Research Workshop on Magnetism and Structure in Systems of Reduced Dimensions, Cargese, France, 15–19 June 1992*, NATO ASI, Ser. B, Vol. 309 (Plenum, New York, 1993), p. 201.
- [9] B. Lairson and B. Clemens, *Appl. Phys. Lett.* (to be published).
- [10] P.M. Oppeneer, J. Sticht, T. Maurer, and J. Kübler, *Phys. Rev. B* **45**, 10 924 (1992).
- [11] T. Massalski, *Binary Alloy Phase Diagrams* (American Society for Metals, Metals Park, OH, 1990), Vol. 2.
- [12] J.M. Sanchez, J.L. Morán-López, C. Leroux, and M.C. Cadeville, *J. Phys. Condens. Matter* **1**, 491 (1989); G. Inden, *Mater. Res. Soc. Symp. Proc.* **19**, 175 (1983).
- [13] R.F.C. Farrow, G.R. Harp, R.F. Marks, T.A. Rabedeau, M.F. Toney, R.J. Savoy, D. Weller, and S.S.P. Parkin, *J. Cryst. Growth* (to be published).
- [14] H. Brändle, D. Weller, S.S.P. Parkin, J.C. Scott, P. Fumagalli, W. Reim, R.J. Gambino, R. Ruf, and G. Güntherodt, *Phys. Rev. B* **46**, 13 889 (1992).
- [15] M.T. Sebastian and P. Krishna, *Phys. Status Solidi (a)* **101**, 329 (1987). Strictly, this model applies to the hcp to fcc transition of a chemically homogeneous sample. However, the model provides a reasonable approximation to the scattering along $(10q_z)$ of alloy films with nearly random in-plane chemical order. Similar fcc fractions are obtained through comparison of the fcc and hcp peak integrated areas.
- [16] F. Bolzoni, F. Leccabue, R. Panizzieri, and L. Pareti, *IEEE Trans. Mag.* **20**, 1625 (1984).
- [17] These measurements were performed at beam line x20c of the National Synchrotron Light Source, Brookhaven, New York.
- [18] C.M. Wayman, in *Physical Metallurgy*, edited by R.W. Cahn and P. Haasen (North-Holland, New York, 1984), pp. 1031–1074.
- [19] At very low deposition temperatures the kinetics limit even MBE growth as evidenced by the fcc inclusions and the absence of chemical ordering in the 450 K film.
- [20] H. Brändle, D. Weller, J.C. Scott, S.S.P. Parkin, and C.-J. Lin, *IEEE Trans. Mag.* **28**, 2967 (1992).
- [21] B.E. Warren, *X-ray Diffraction* (Dover Publications, Inc., New York, 1990), p. 208. S is defined as $(r_{\text{Pt}} - x_{\text{Pt}})/y_{\text{Co}}$ where r_{Pt} is the fraction of Pt sites correctly occupied, x_{Pt} is the Pt sample fraction, and y_{Co} is the fraction of Co sites in the perfectly ordered alloy. We assume the perfectly ordered alloy consists of alternating CoCo and CoPt planes. This structure can be represented as two hexagonal sublattices, one containing only Co and the other consisting of alternating layers of Co and Pt. We apply the definition of S to the CoPt sublattice. With this definition $S = 1$ for Co_3Pt with perfect layerwise chemical order while $S = 0$ for complete chemical disorder. By applying the definition of S to only the CoPt sublattice, S is sensitive only to layerwise chemical order and not to in-plane chemical order.